High-Temperature Sapphire Pressure Sensors For Harsh Environments

Haocheng Zhou[1], Austin Vera[1], Peter Woerner[2], Jakob Consoliver[2], Alexandra Garraud[1], David Mills[1], William Oates[2], Mark Sheplak[1]

[1]Interdisciplinary Microsystems Group, University of Florida
[2]Florida State University

4/12/2018

DE-FE0012370 - 01/01/2014 – 08/31/2018
2018NETL Crosscutting Research Review Meeting

Project Information

- Focus: Development of novel machining methods for the fabrication of harsh environment pressure sensors
- Award information
  - Project title: “High-temperature sapphire pressure sensors for harsh environments”
  - Award #: DE-FE0012370
  - Program manager: Sydni Credle
  - Duration: 3 years (1.5 year NCE) started Jan 2014
- Project team
  - University of Florida
  - Florida State University

Outline

- **Introduction**
- Thermal Damage Modeling (FSU)
- Sensor Fabrication (UF)
- Acoustic Characterization (UF)

Motivation

- Next generation advanced energy systems will require harsh environment dynamic instrumentation:
  - Process control/closed loop feedback
  - Increase efficiency, reduce emissions & cost
- Sensor operational requirements
  - Temperature: >1000 °C and dynamic pressure: up to 1000 psi, 10s kHz
  - Atmosphere: corrosive and/or erosive
- Conventional pressure sensor instrumentation limited to ~500 °C
  - Temperature mitigation techniques: stand-off tubes, water cooling
  - Oxsensis claims 750 °C using sapphire interferometry technique

Technical Objectives

- Novel sapphire fabrication processes
  - Subtractive machining: ultrashort pulse laser micromachining
  - Additive manufacturing: thermocompression bonding via spark plasma sintering
- Modeling and characterization of laser machined sapphire
  - High temperature experimental characterization, modeling, and Bayesian uncertainty quantification
- Fabricate, package, calibrate, and demonstrate sapphire optical pressure sensor

Previous Work

- Sapphire fabrication processes
  - Developed empirical based path planning simulation for pico-second laser micromachining
  - Proved concept of thermal compression bonding via spark plasma sintering
- Modeling and characterization of laser machined sapphire
  - High temperature (1500^{o}C) bend bar characterization
  - Light-matter ablation physics and Bayesian uncertainty quantification
- Fabricated various pressure sensor components

Outline

- Introduction
- **Thermal Damage Modeling (FSU)**
- Sensor Fabrication (UF)
- Acoustic Characterization (UF)

Nanoindentation analysis

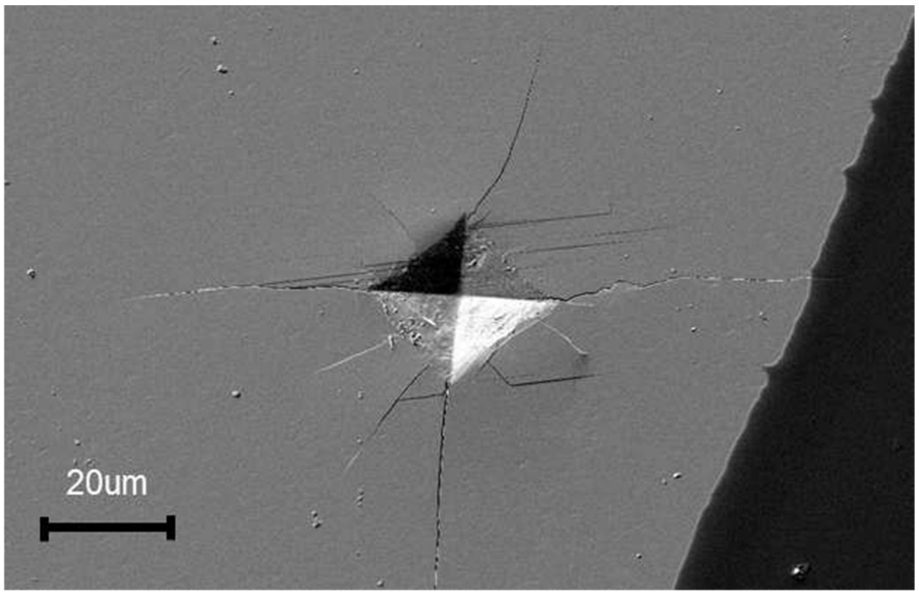

Pristine Sapphire

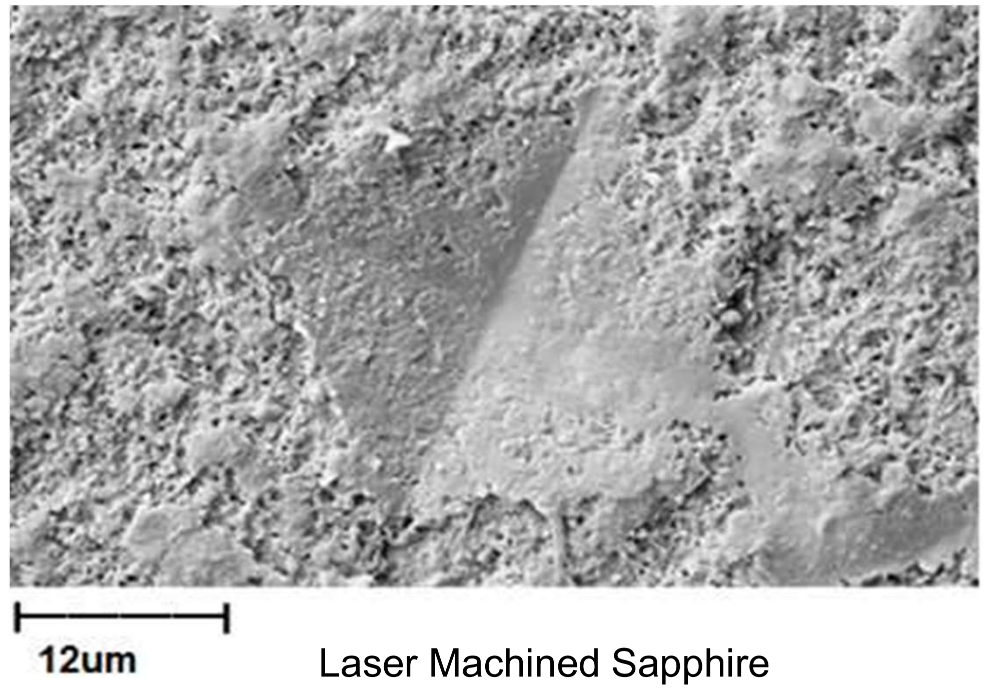

Laser Machined Sapphire

Justin Collins, William S Oates, Mark Sheplak, and Daniel Blood. Experimental investigation and modelling of laser machining of sapphire for high temperature pressure transducers. In 56th AIAA/ASCE/AHS/ASC Structures, Structural Dynamics, and Materials Conference, page 1120, 2015.

Nanoindentations: Experimental Results

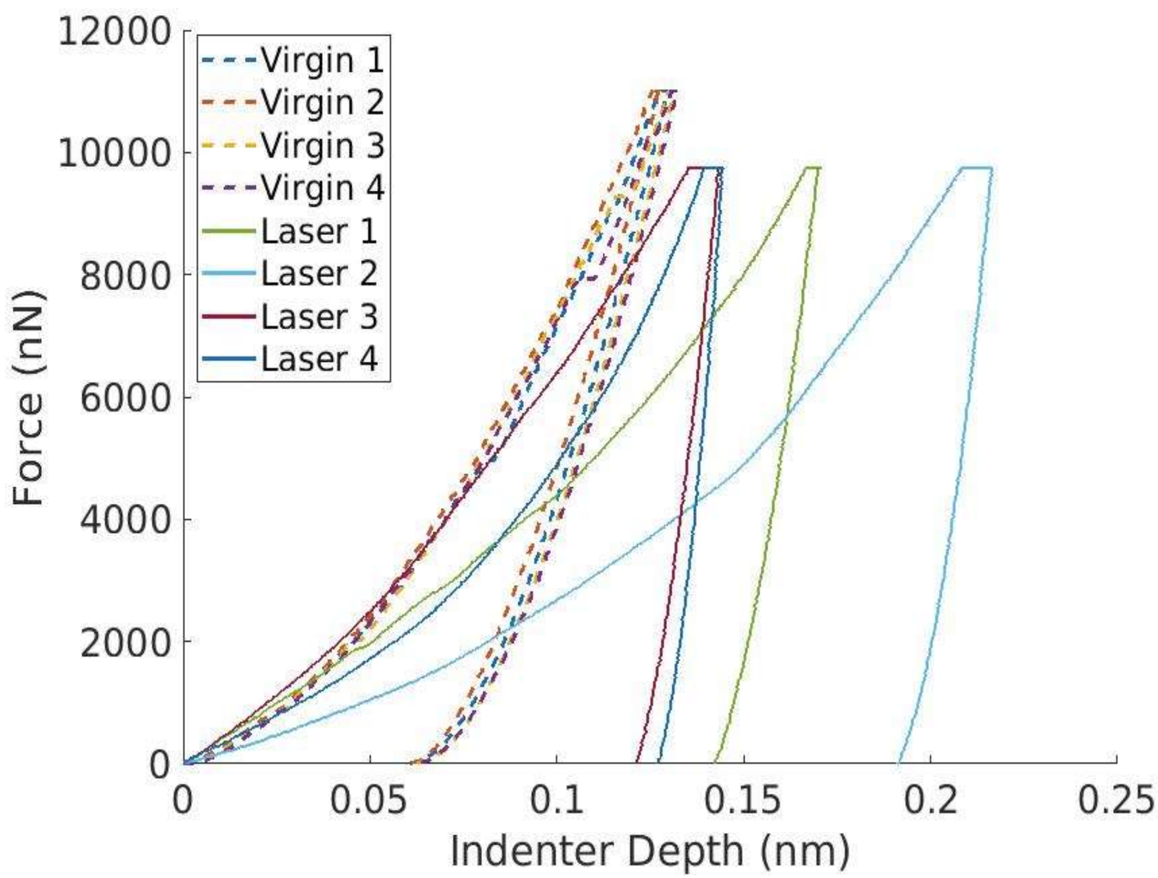

Finite Deformation FEA Modeling

Deformation Decomposition

$$\mathbf{F} = \mathbf{F}^{p} \cdot \mathbf{F}^{e}$$

Stress-Strain Relation

$$\mathbf{S} = \mathbf{C} : \mathbf{E}^{e}$$

C - Isotropic elastic moduli

Yield Stress Evolution

$$Y(e^p) = Y_0 + H_{iso} e^p$$

Assume plasticity law with hardening

- Amorphous zone near surface
- No distinct dislocation pattern

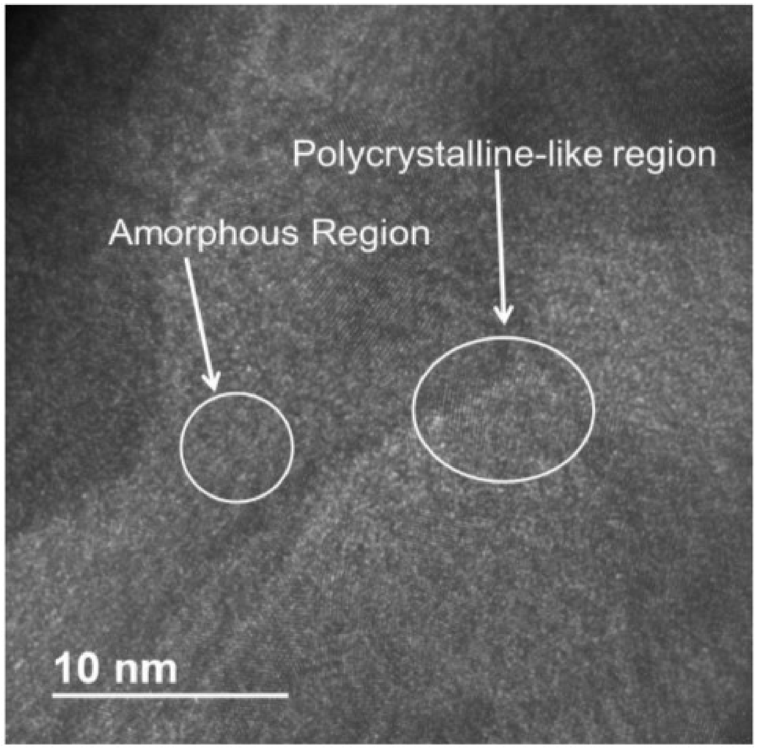

Justin Collins, William S Oates, Mark Sheplak, and Daniel Blood. Experimental investigation and modelling of laser machining of sapphire for high temperature pressure transducers. In 56th AIAA/ASCE/AHS/ASC Structures, Structural Dynamics, and Materials Conference, page 1120, 2015.

Key Results

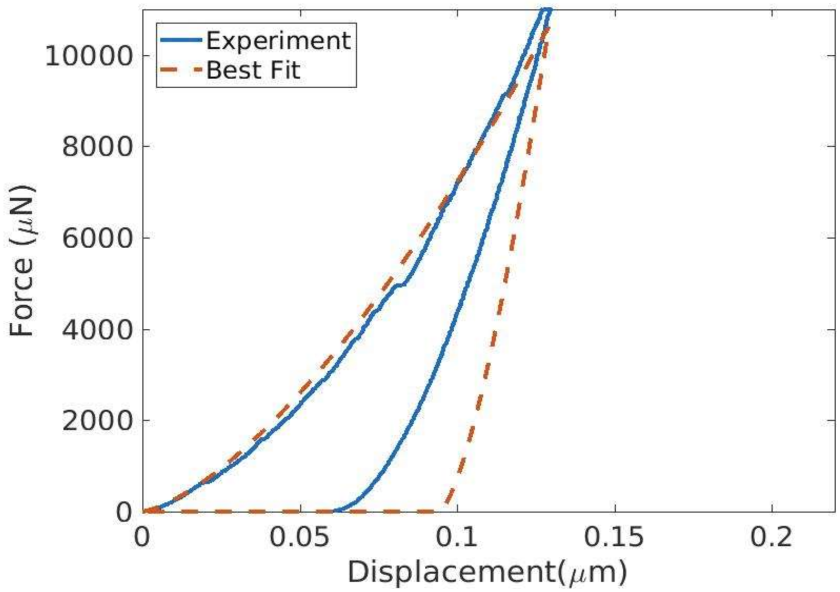

Virgin Sapphire

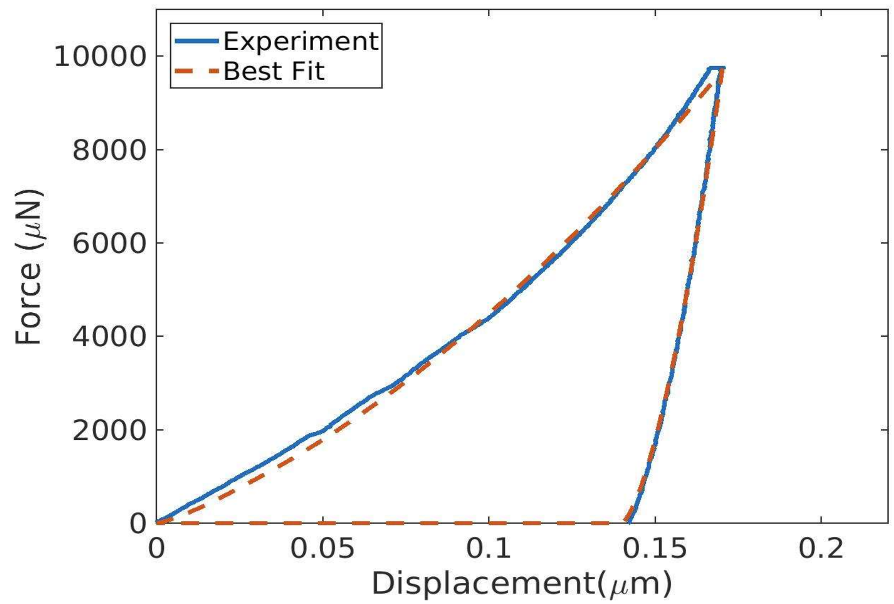

Laser Machined Sapphire

Plastic Hardening Parameter Relations

Experiment	Linear Hardening Parameter (MPa)
Virgin 1	60
Laser Machine 1	28
Laser Machine 2	19
Laser Machine 3	46
Laser Machine 4	37

Model fits apply E = 450 GPa, Yield Stress = 1 MPa

Sapphire Crystal Structure

- Specimens cut with r-plane normal to surface.
  - ϕ_0 :angle between specimen normal and r-plane surface normal
  - Assumes uncertainty in crystal cut & x-ray measurements
- X-ray diffraction scans were done in the pristine and laser machined regions
  - Both normal and in-plane measurements were taken

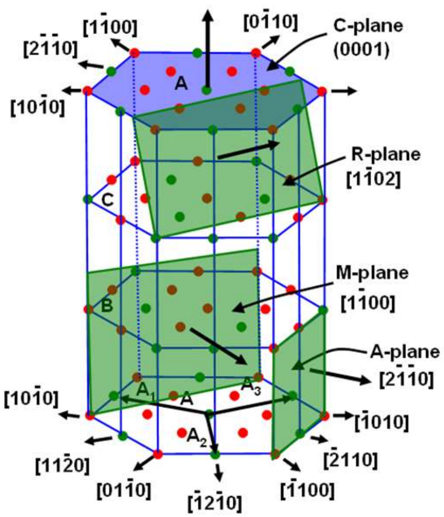

Figure 1: Sapphire crystal structure

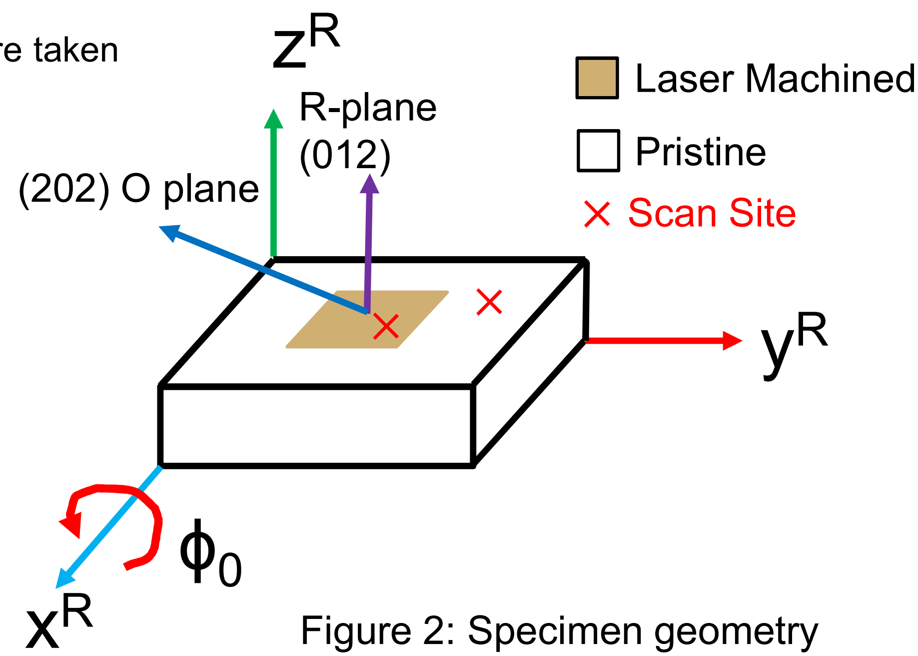

Figure 2: Specimen geometry

X-Ray Diffraction

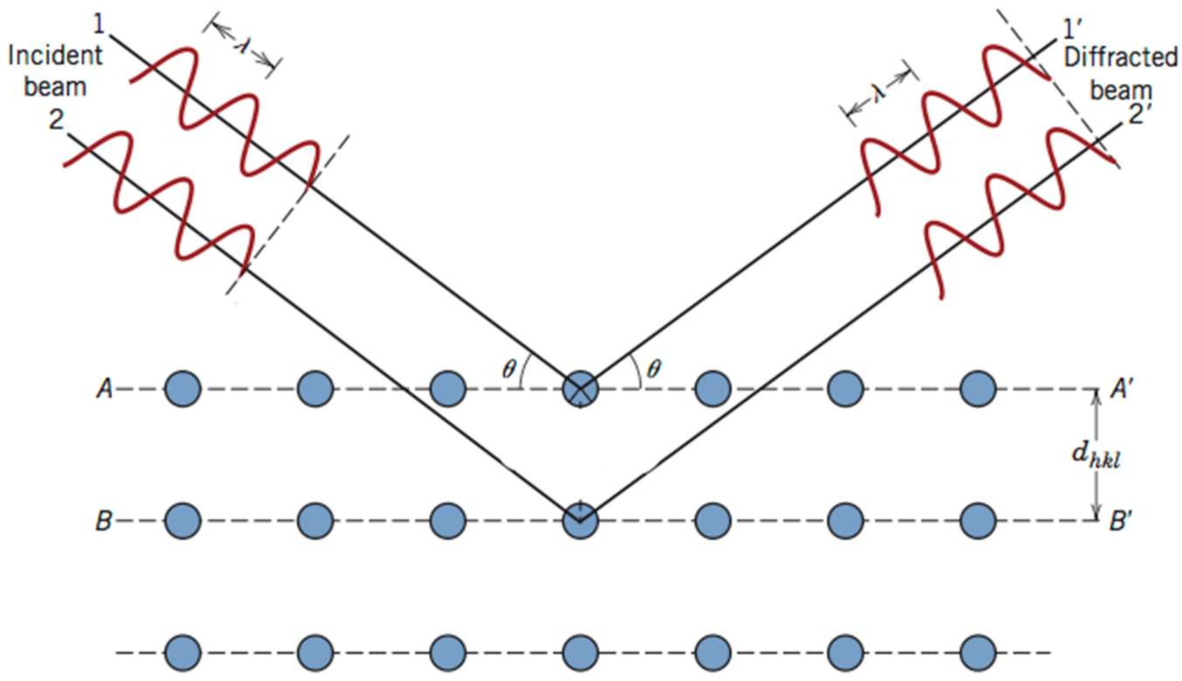

Figure 3: Diffraction of x-rays by planes of atoms.

$$d_{hkl} = \frac{\lambda}{2 \sin \theta}$$

Normal (r-plane) Peak Comparisons

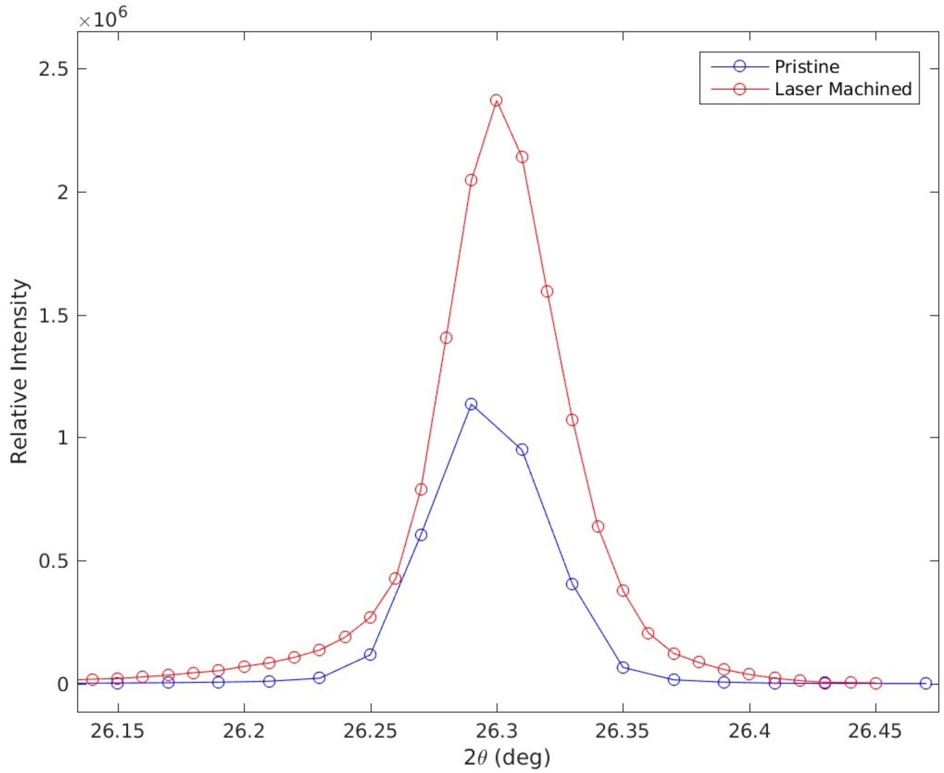

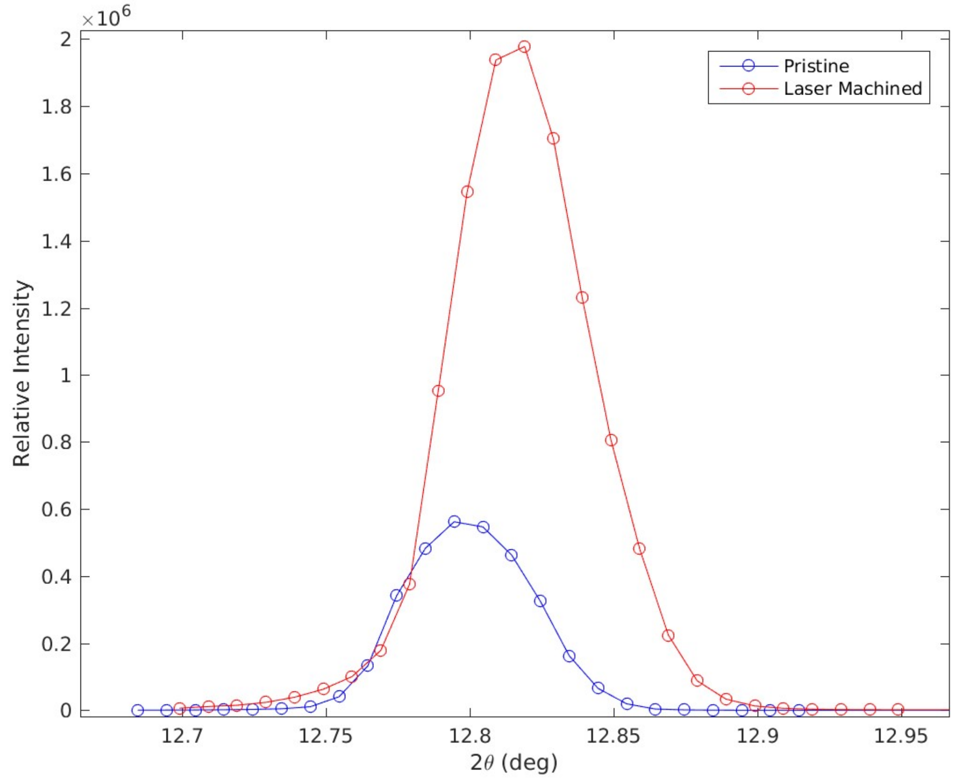

X-Ray Kinematic Model

$$I = |F_{hkl}|^2 = \left(\sum_{i=1}^{N} f_i e^{2\pi i (\mathbf{P_j} \cdot \mathbf{x_i} \cdot \mathbf{R}(\varphi_0))} \right)^2$$

f_i : Scattering factor
P_j : Miller indices (hkl) of plane of interest j
x_i : Cartesian coordinates of atom i
$R(\phi_0)$: Rotation Matrix dependent on ϕ_0
N: number of atoms

$$I(\theta) = |F_{hkl}|^2 G(\theta) = I_{scale} |F_{hkl}|^2 e^{-\sqrt{2\pi}\frac{(\theta-\theta_b)^2}{2\sigma^2}}$$

θ: Angle of incident x-ray
θ_b: Angle at which maximum intensity occurs (Bragg Angle)
σ : Standard deviation of peak about θ_b
I_{scale}: Scaling factor

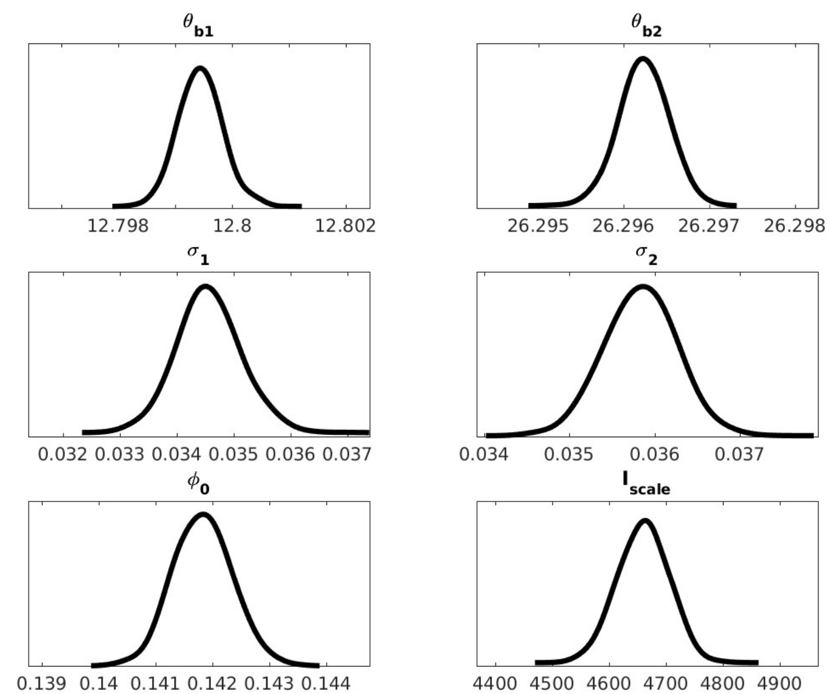

Parameter uncertainty quantified using Bayesian statistics

- Markov Chain Monte Carlo algorithm
- Delayed Rejection Adaptive Metropolis (DRAM)

Spectra Predictions Normal (012) to R-Plane (Pristine Sapphire)

Normal (012) to r-plane

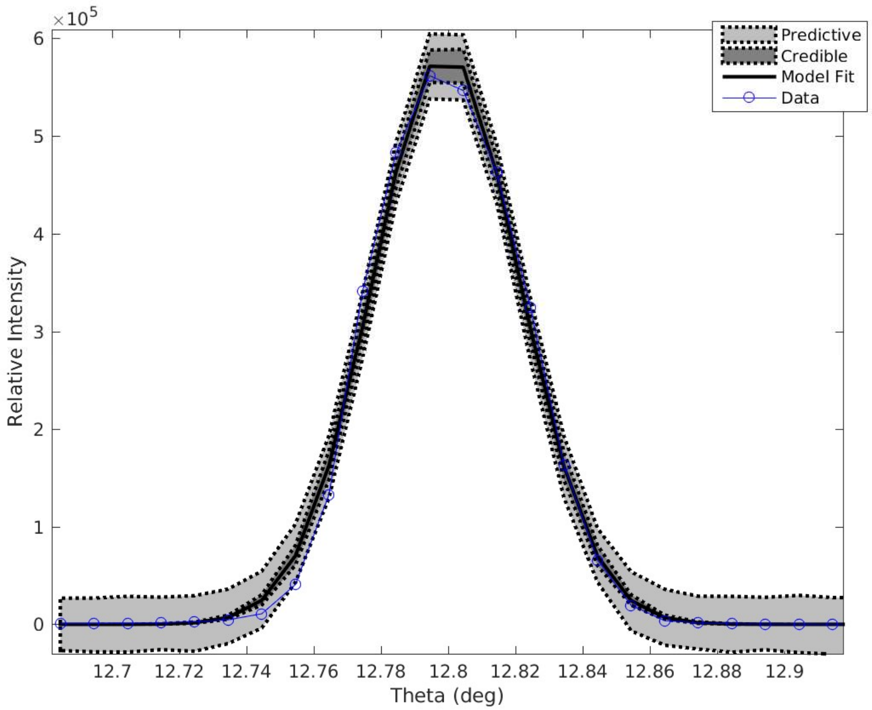

Normal (202) plane

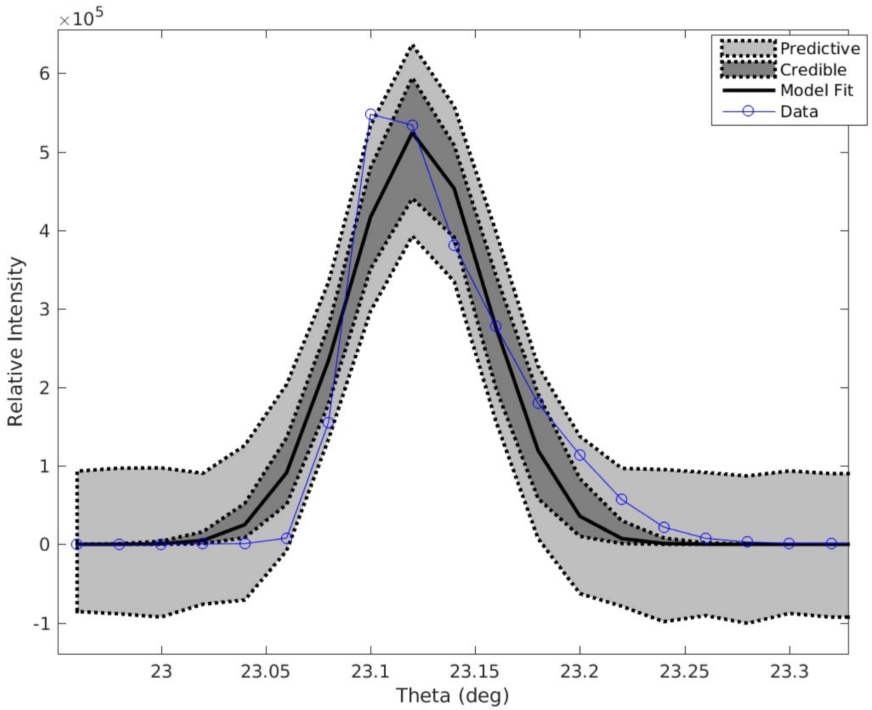

Strain Inference from X-Ray Spectra

$$\epsilon_{hkl} = \frac{\sin\theta_{pristine} - \sin\theta_{laser}}{\sin\theta_{laser}}$$

Equation to calculate strain in (hkl) plane direction

$$\epsilon^R = \begin{bmatrix} ? & ? & ? \\ X & ? & ? \\ X & X & \epsilon^R_{33} \end{bmatrix}$$

Strain tensor relative to R coordinate system (x^R,y^R,z^R)

- ϵ^R_{33} = (-1.366 ± 0.019)·10^{-3} (90% credible interval)

$$\epsilon^O = \begin{bmatrix} A^O & C^O & D^O \\ C^O & B^O & E^O \\ D^O & E^O & \epsilon^O_{33} \end{bmatrix}$$

Strain tensor relative to O coordinate system (x^O,y^O,z^O)

- ϵ^O_{33} = (-0.098 ± 0.922)·10^{-3} (90% credible interval)
- A^O, B^O, C^O, D^O, and E^O are unknown parameters

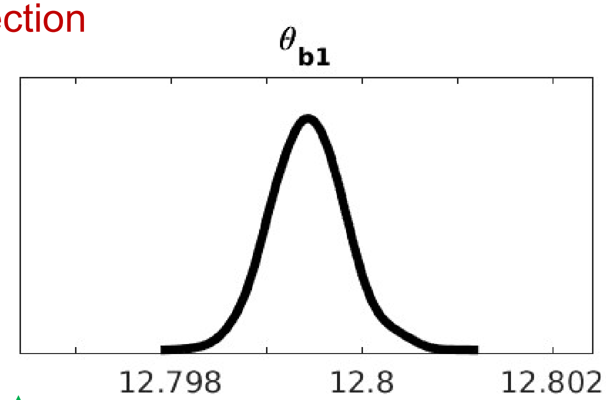

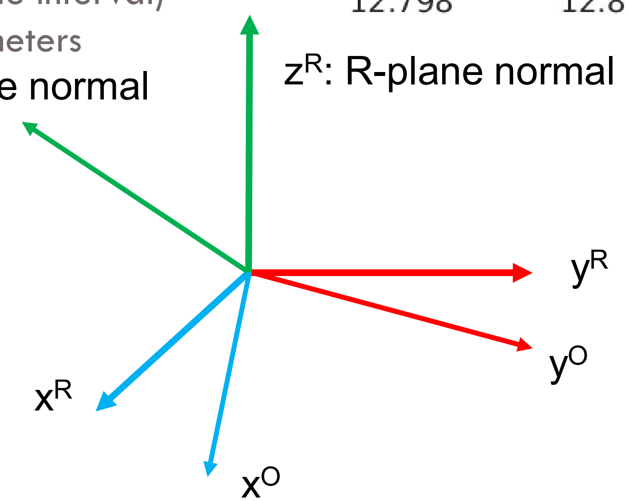

If $\boldsymbol{\varepsilon}^O$ is rotated from the O coordinate system to the R then: $\bar{\boldsymbol{\varepsilon}}^O = \boldsymbol{\varepsilon}^R$

Model Assumptions

- Unknown strain parameters inferred using:

$$t_i = \sigma_{ji} n_j^R = 0$$

$$\mathbf{n}^R = \mathbf{i}_z$$

$$\sigma_{ij} = C_{ijkl}\left(\varepsilon_{kl} - \varepsilon_{kl}^{\text{Pristine}}\right) \cong C_{ijkl}\varepsilon_{kl}$$

Assumptions:

1. Pristine reference state has zero residual strain
2. Traction on r-plane is zero
3. $\varepsilon_{11}=\varepsilon_{22}$ and modulus is isotropic

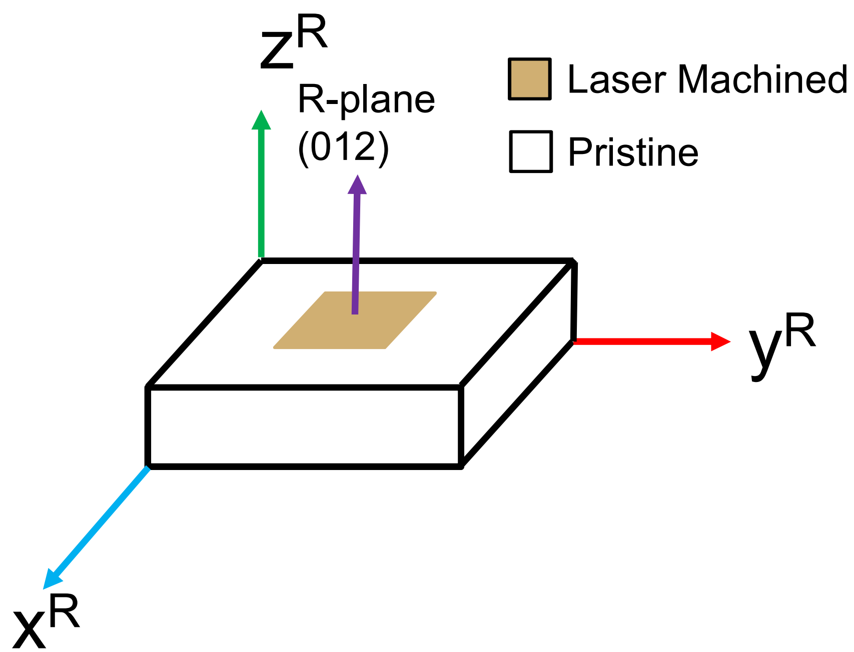

Residual Strain Estimations

Assuming isotropy ($\epsilon^R_{11} = \epsilon^R_{22}$) and the relation $\epsilon^O_{33} = \epsilon^R_{33}$ = const.

- $D^O = f(A^O, B^O)$
- $E^O = f(A^O, B^O, C^O)$

Using Bayesian methods coupled with the above relations the strain tensor is determined:

$$\epsilon^R = \begin{bmatrix} 4.4 & 2.1 & -1.2 \\ 2.1 & 4.4 & -7.6 \\ -1.2 & -7.6 & -1.4 \end{bmatrix} \cdot 10^{-3}$$

Where:

$\epsilon^R_{11} = \epsilon^R_{22} = (4.447 \pm 0.530)\cdot 10^{-3}$

$\epsilon^R_{33} = (-1.366 \pm 0.019)\cdot 10^{-3}$

High confidence laser machined zone has in-plane compression which produces higher toughness

Outline

- Introduction
- Thermal Damage Modeling (FSU)
- **Sensor Fabrication (UF)**
- Acoustic Characterization (UF)

Transduction Mechanism Selection

	Capacitive	Piezoresistive	Piezoelectric	Optical
Thermal drift elimination	✓	X	✓	✓
DC measurement	✓	✓	X	✓
EMI insensitivity	X	X	X	✓
Harsh environment capability (>500 °C)	X	X	X	✓
Packaging simplicity	X	X	X	X

- Optical transduction (intensity modulation – optical lever) is selected given the constraints

Pro	Con
Incoherent source	Lower sensitivity
Thermally stable	

Material Selection

	Silicon Carbide	Diamond	Sapphire
Bulk substrate availability	✓	X	✓
Optical fiber availability	X	X	✓
Well-established μ-machining processes	X	X	X

- Benefits of sapphire
  - High melting point (2053 °C)
  - Resistance to chemical corrosion
  - Excellent hardness
  - Large transmission window (200 nm – 5 μm)
  - Multimode optical fibers available

Sensor Fabrication – Mechanical Sensitivity Optimization

- Aim: optimize diaphragm diameter for best acousto-mechanical sensitivity using lumped element modeling:

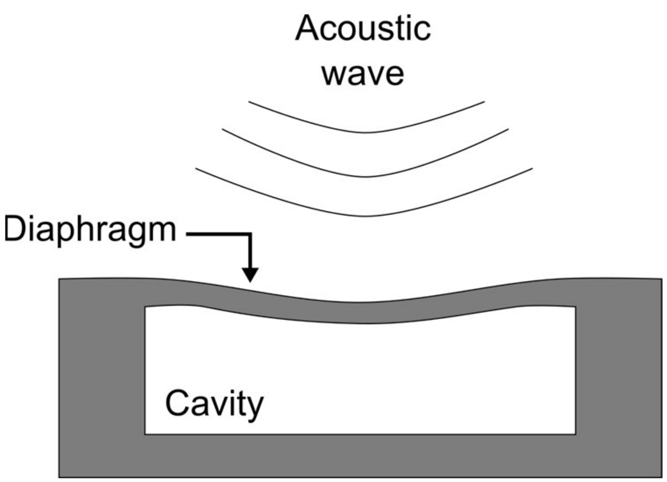

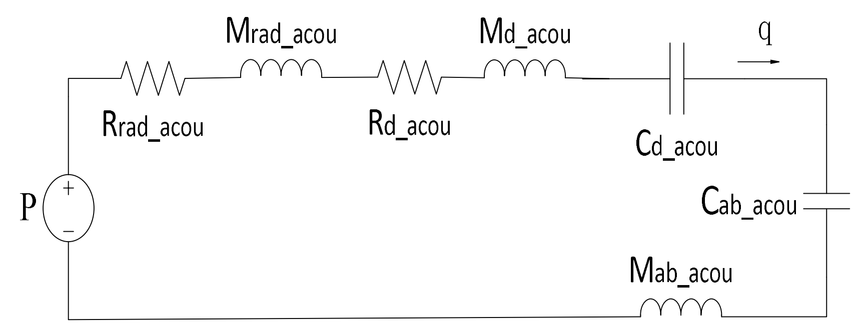

Sensor Fabrication – Mechanical Sensitivity Optimization

- Aim: optimize diaphragm diameter for best acousto-mechanical sensitivity
- Using lumped element modeling
- Assuming 200 kPa_{max}, and a 38 ± 22 μm thick substrate, f_{mincon} solutions:

Thickness (μm)	Diameter (mm)	Flat-band Sensitivity S_{AM} (nm/Pa)	Flat-band Sensitivity S_{AM} (dB)	Maximum deflection (μm)	Resonating Frequency (kHz)
60	5.4	1.2×10^{-1}	-198.2	24.5	31.3
50	4.4	9.3×10^{-2}	-200.6	18.7	38.1
38	3.4	7.6×10^{-2}	-202.4	15.1	46.0
16	1.4	2.9×10^{-2}	-210.7	5.8	90.7

Design diameter choosen = 5 mm

Sensor Fabrication – Optical Sensitivity Optimization

- Aim: Find the distance between end of fiber and reflective Pt layer for linear optical response

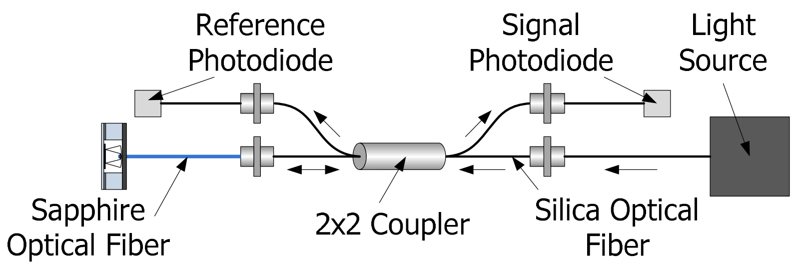

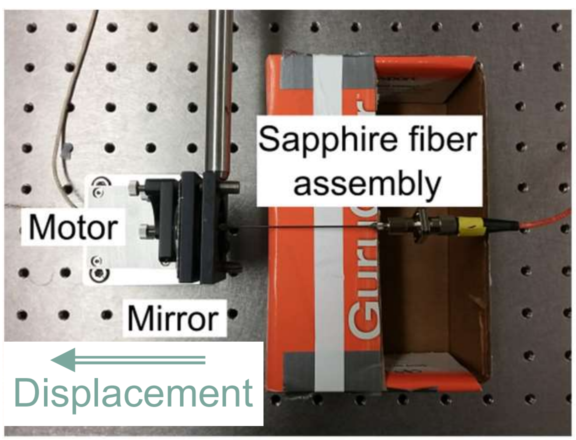

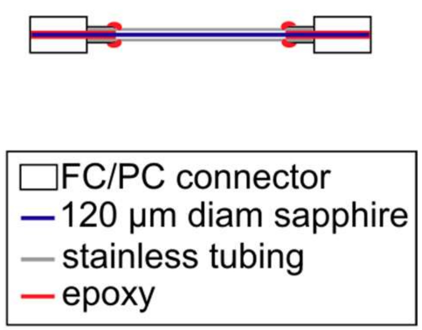

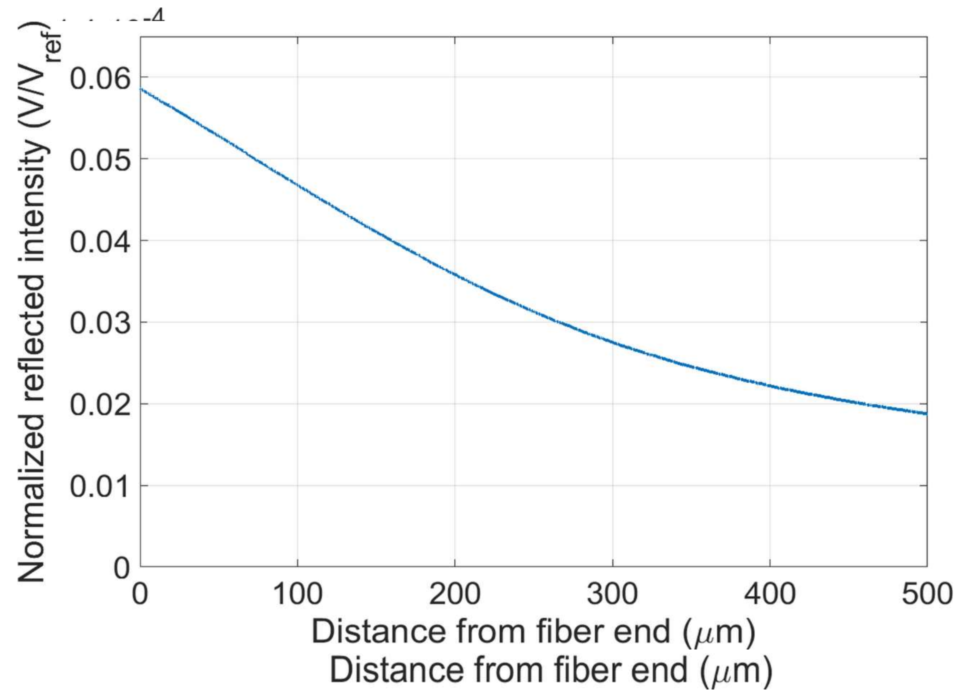

Sensor Fabrication – Initial Process Flow

→ Issue:
Thermocompression bonding tool is down
→ Solution:
Use of ceramic epoxy for bonding the two substrates together

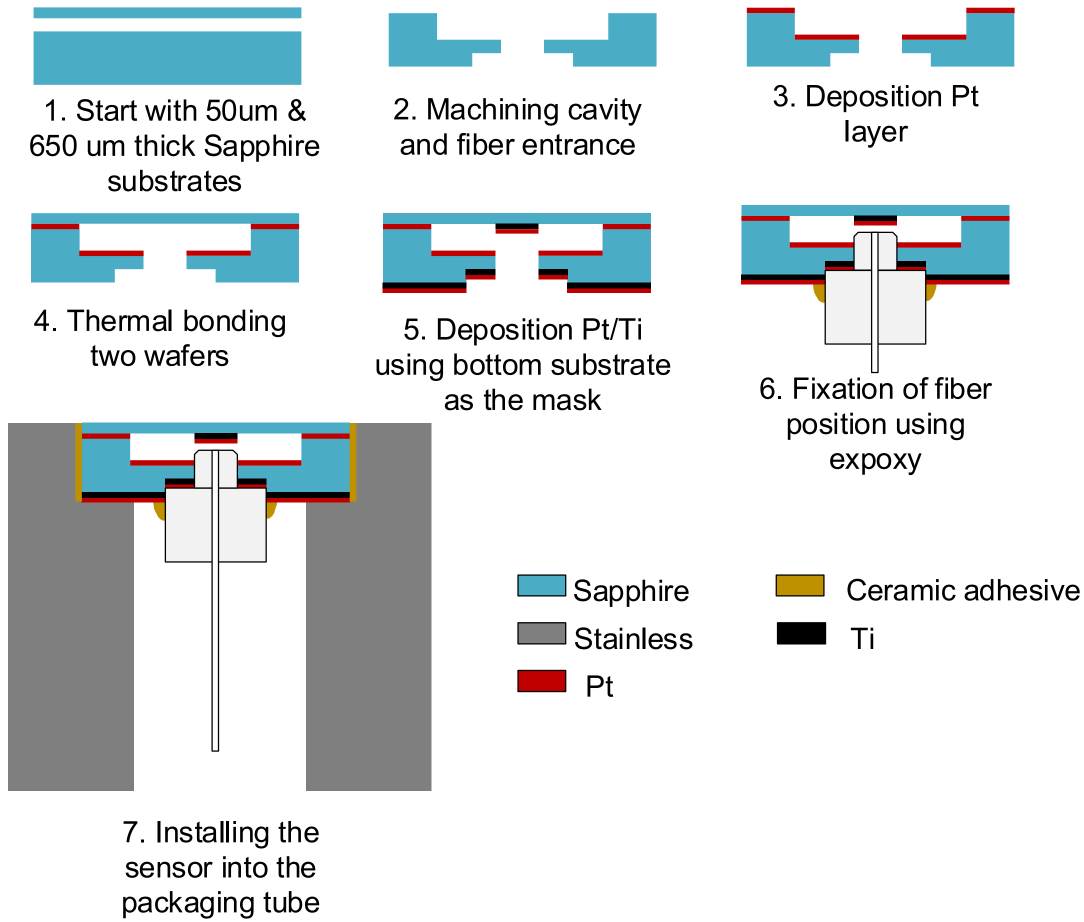

Sensor Fabrication – Revised Process Flow

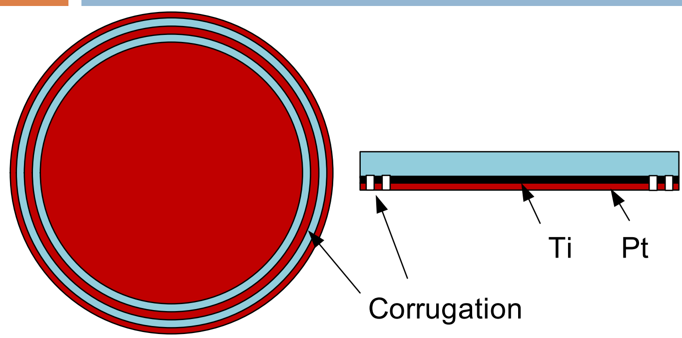

1. Diaphragm substrate (8mm) with deposited Ti/Pt film and laser machined corrugation around edge

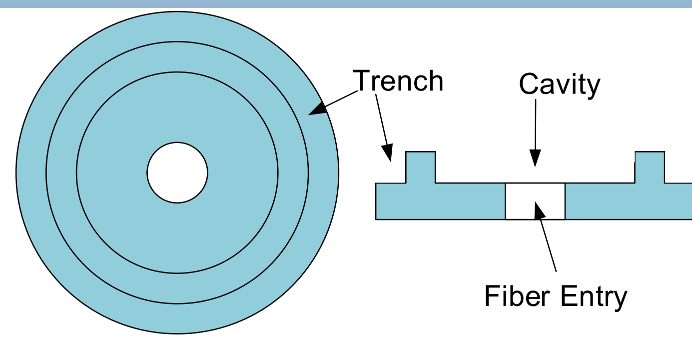

2. Cavity substrate (8mm) with laser machined cavity (5mm) and optical entry hole

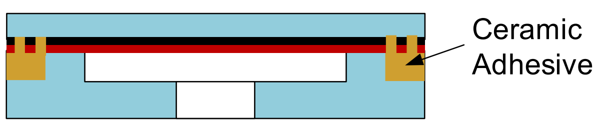

3. Bonding two substrates using ceramic adhesive on the edge trench

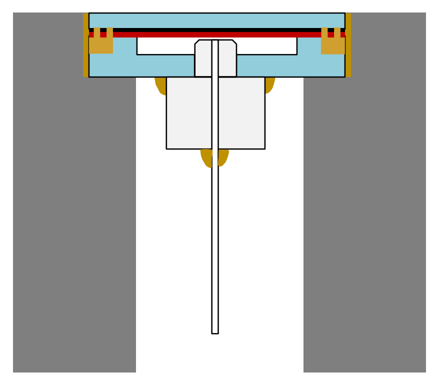

4 Installing the sensor into the packaging tube

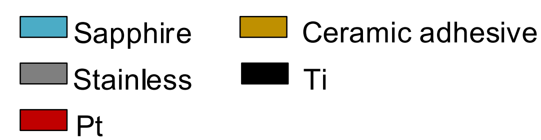

Sensor Fabrication – Bonding

- Laser machining for both substrates
- Laser machining corrugation for adhesion improvement

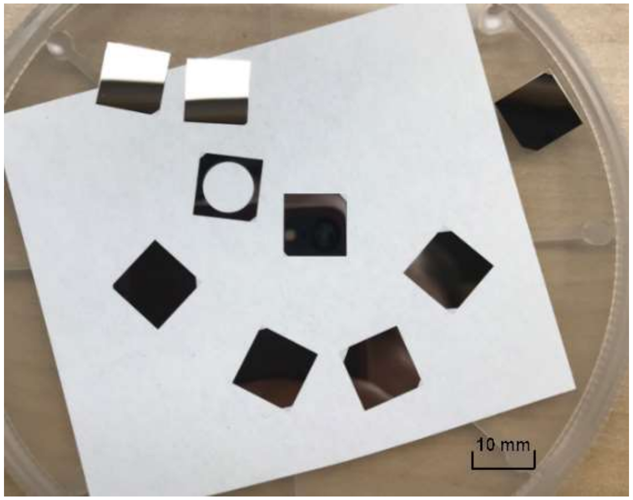

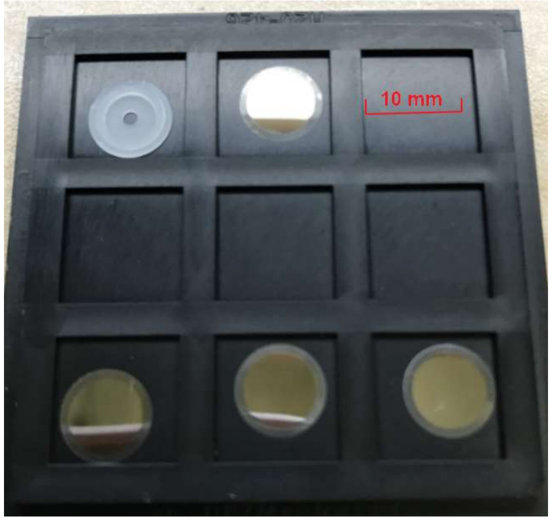

Microscope 100X

Sensor Fabrication – Membrane/Cavity Substrates

- Alignment on flip-chip bonder
- Manual application of alumina ceramic adhesive into the edge trench

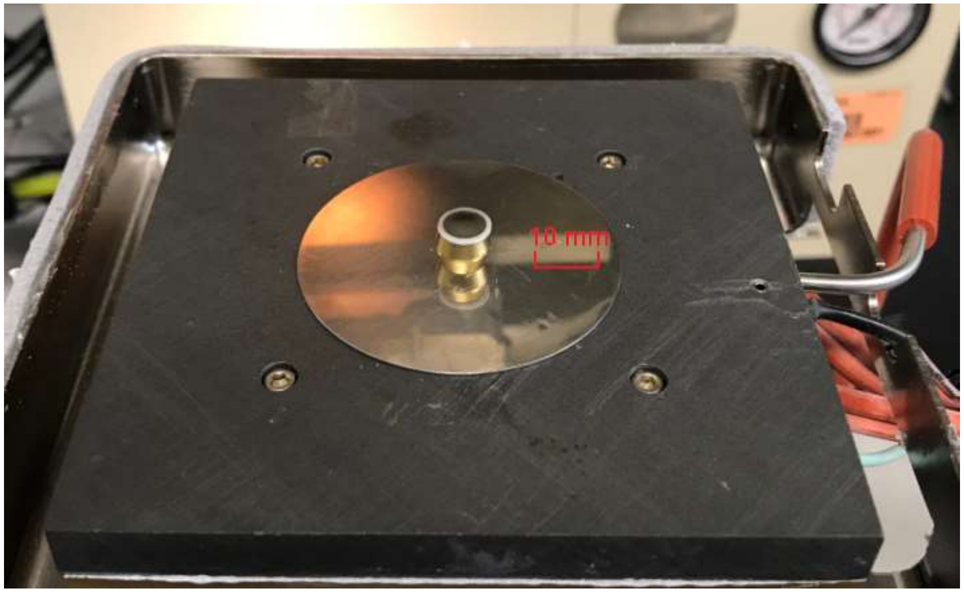

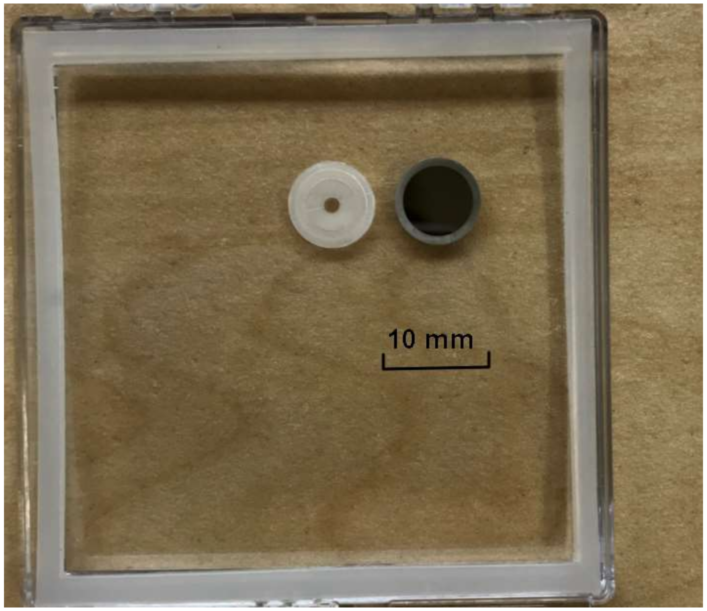

Sensor Fabrication – Optic Fiber Structure

- Sapphire optic fiber was mounted on:
  - Laser micromachined stepped ferrule
  - FC connector
  - Stainless steel 304 tubing for rigidity
  - High-temperature alumina ceramic adhesive for bonding

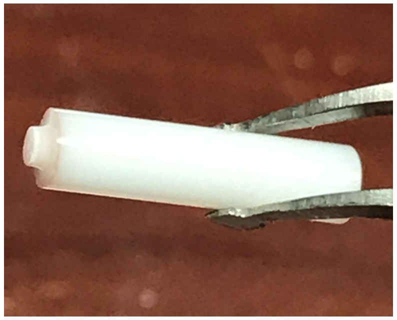

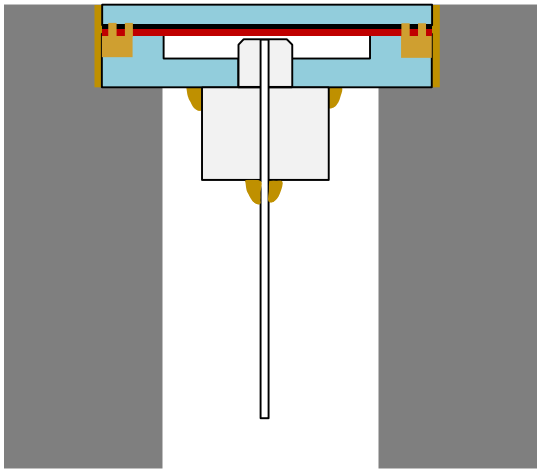

Sensor Fabrication – Packaging

- Stainless steel housing
- High-temperature alumina ceramic adhesive for bonding

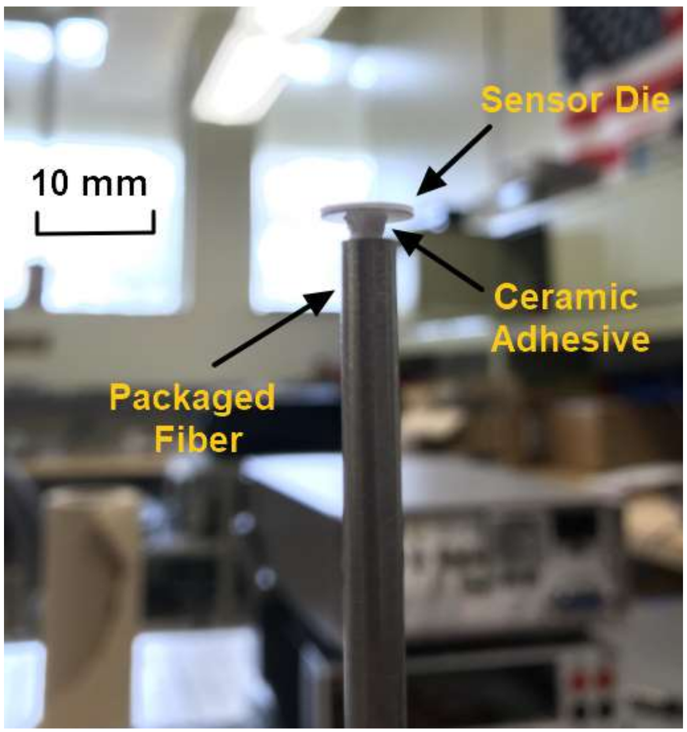

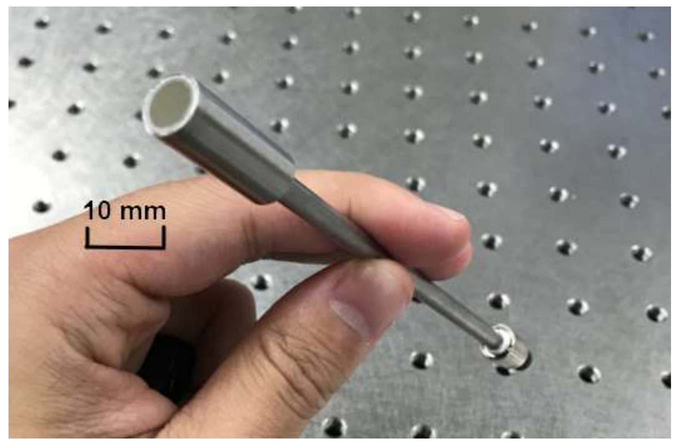

Outline

- Introduction
- Thermal Damage Modeling (FSU)
- Sensor Fabrication (UF)
- **Acoustic Characterization (UF)**

High Temperature Testing Facility

- Plane Wave Tube (PWT) for acoustic characterization
  - Speaker generates acoustic pressure waves
  - Propagate as plane acoustic waves through the tube furnace
  - Option: tube furnace ON ➔ high temperature capability
  - Pressure sensor characterized *in situ*

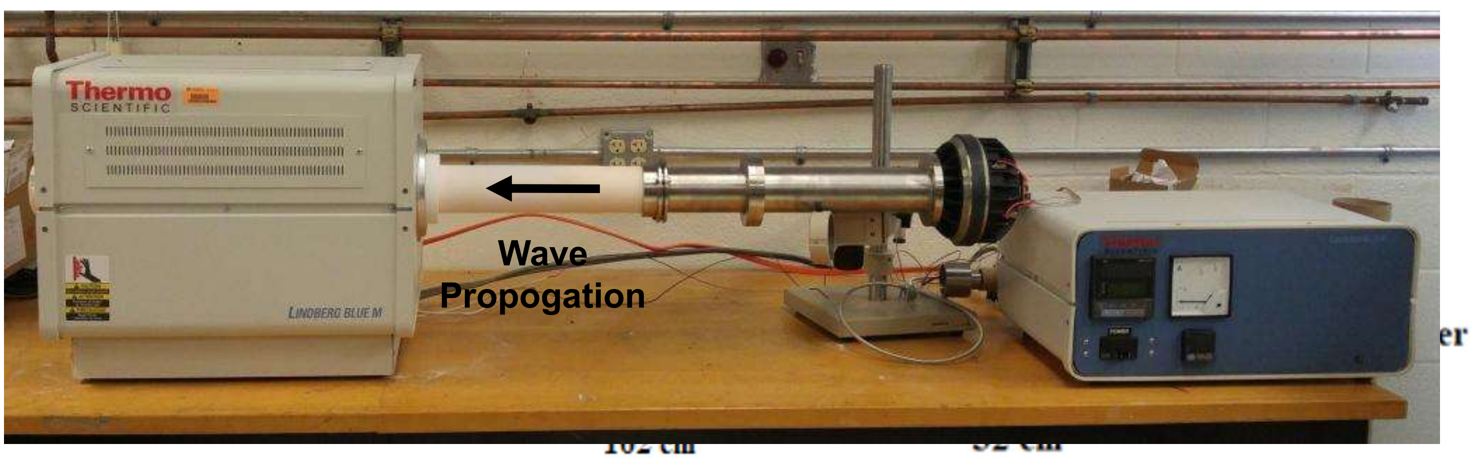

Step 1: Characterization of Temperature

- Aim: acoustic characterization up to 1200 °C
- Issue: measured temperature is too low
- Solution: adding insulation to prevent thermal leak

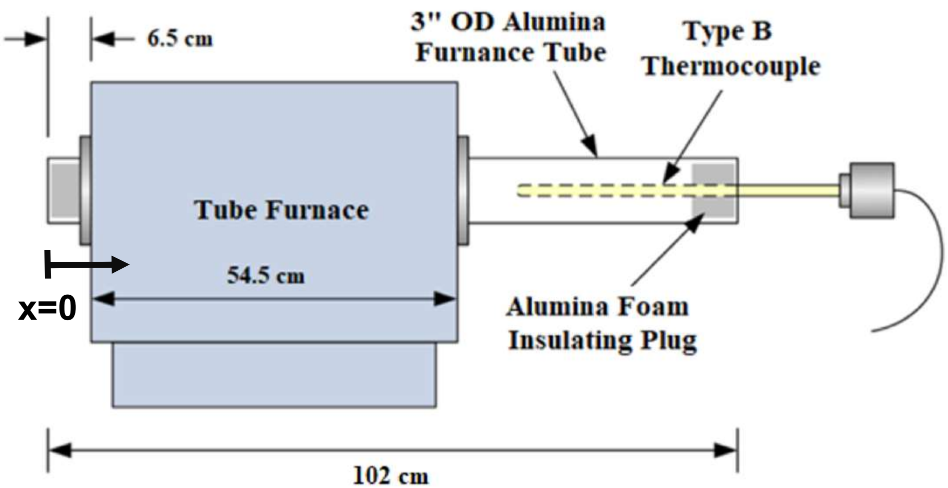

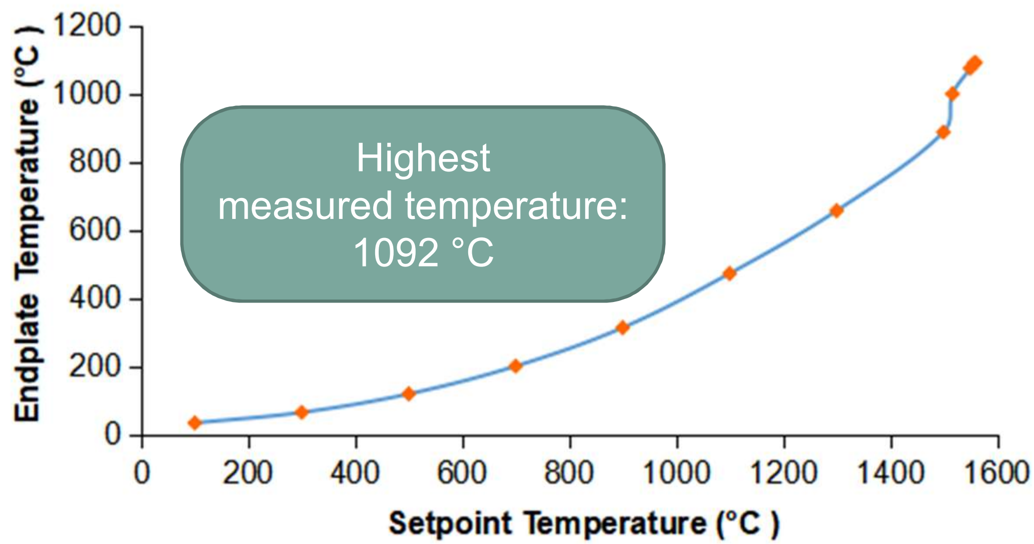

Step 2: Acoustic Characterization

- High temp PWT test set up
- Sensor (DUT,1), probe tip microphone (reference,2), thermocouple(3)

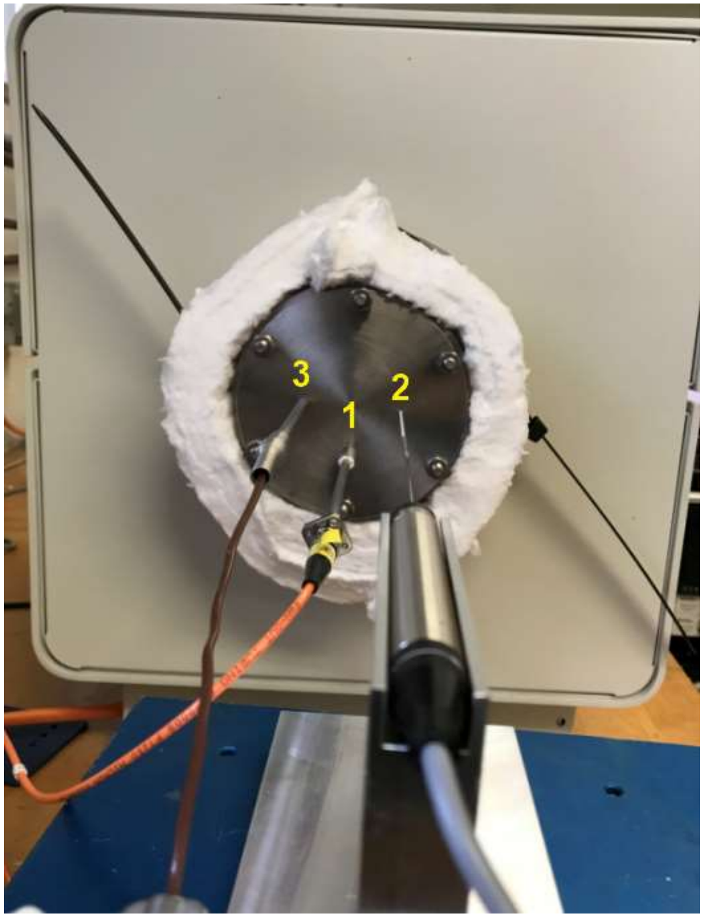

Step 2: Acoustic Characterization Results

- SPL(90-160dB) Sweep at 1kHz
- Temperature from 23°C (room temp) to 600°C with 100°C step size
- Sensitivity drops dramatically after 500°C
  - Failure?

Step 2: Acoustic Characterization Results

- SPL(90-160dB) sweep at 1kHz
- Temperature from 23°C (room temp) to 600°C with 100°C step size
- Sensitivity drops after 500°C

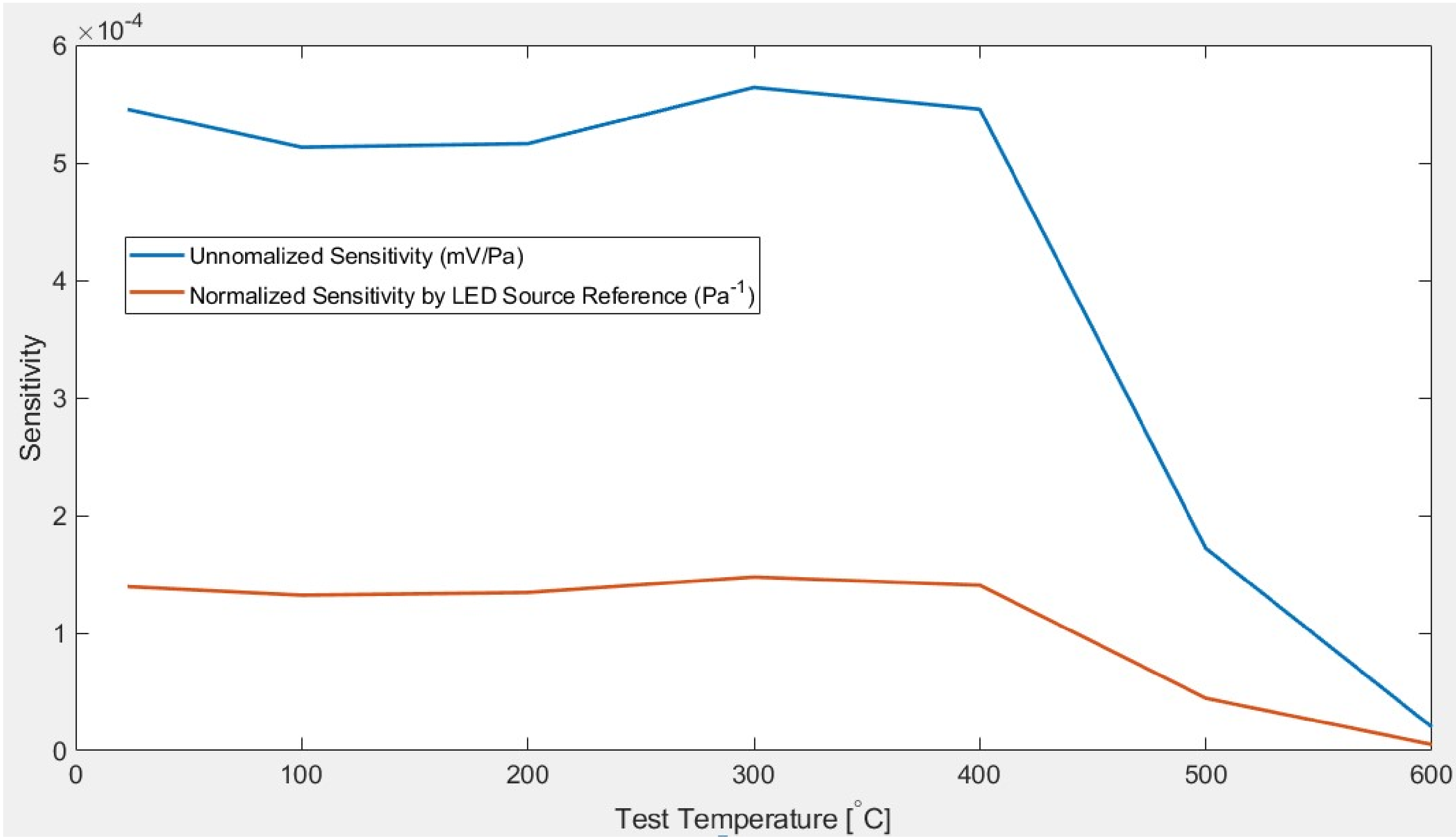

Step 2: Acoustic Characterization Results

- Frequency response function via multisine acoustic waves (300-2200Hz)
- Temperature from 23°C to 600°C
- FRF magnitude drops after 500°C

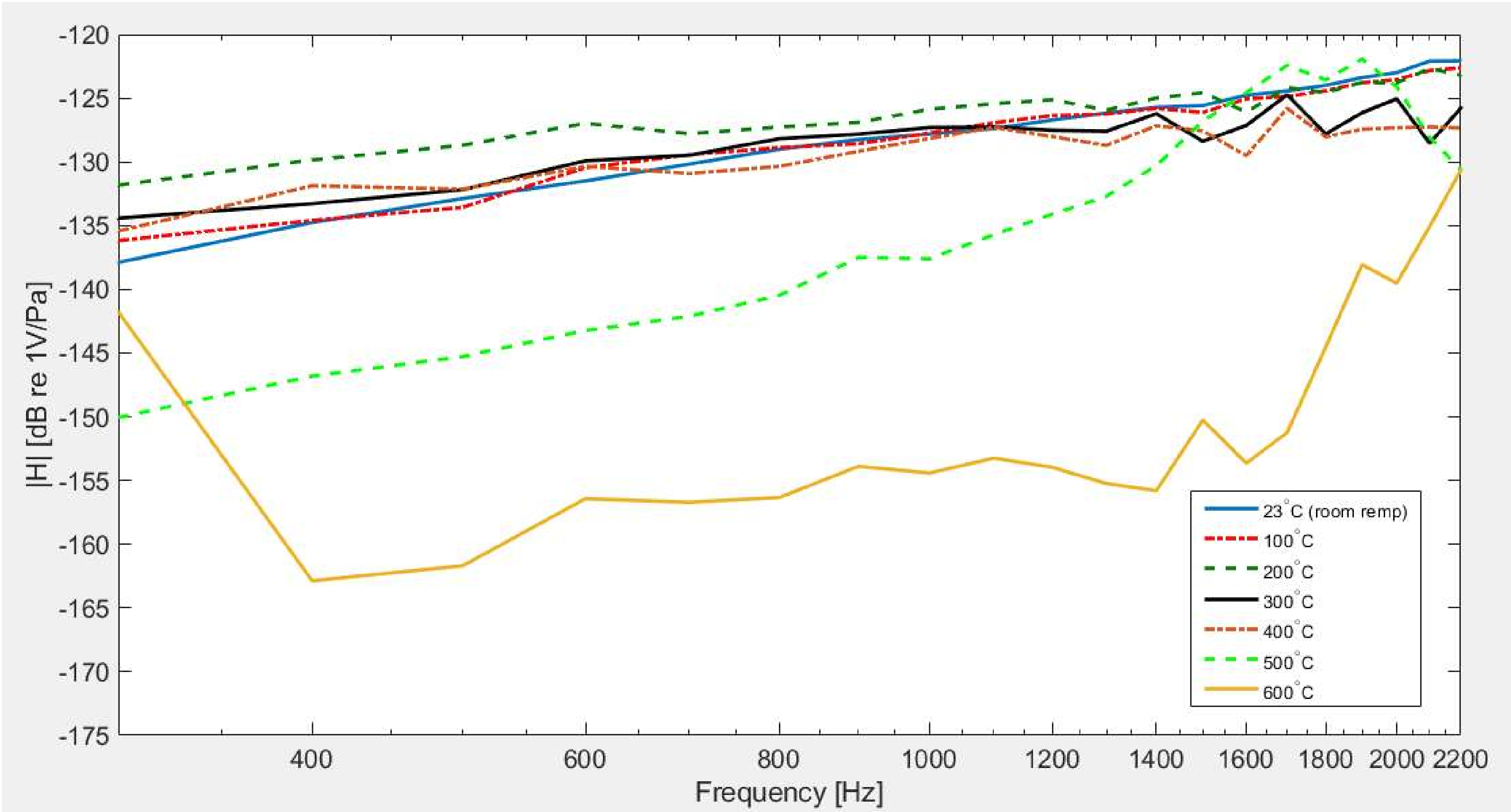

Conclusions

- Material Characterization and Modeling
  - Changes in plasticity of laser machined sapphire quantified using finite deformation contact mechanics & FEA
  - X-ray diffraction and Bayesian UQ used to identify source of increase in fracture toughness--in-plane compression
- Sensor Fabrication
  - Determined the separation between fiber and reflective membrane for optimal sensitivity
  - Designed, fabricated and packaged a prototype sapphire pressure sensor using a ceramic adhesive
- Acoustic Characterization
  - Optimized high temperature plane wave tube setup to reach 1100 °C at sensor location
  - Set up all the equipment necessary for characterization
    - Thermocouple, remote reference microphone with probe tip, sensor
  - Characterized sensor up to 500 °C (failure point)

Future Work

- Additive Manufacturing Process and Mechanics
  - Develop bonding technology to bond sapphire substrates with and without intermediate layers
  - Experimentally characterize bonding strength and fracture as a function of temperature
  - Develop a fundamental understanding of high temperature (>1000C) fracture mechanics and interfacial material physics
  - Understand laser processing parameters on subsurface material properties to enhance fatigue resistance and additive/subtractive manufacturing
- Sensor Fabrication
  - Improve the fabrication and packaging process including thermal compression bonding and packaging sealing
- Acoustic Characterization
  - Calibrate PWT acoustic response at high temperatures for a new sensor with improved fabrication and packaging
  - Hot jet test using high temperature sapphire sensor
  - Test long term stability of the sensor

Questions?

Thank you!